

A PHYSICAL MODEL FOR WIRELESS CHANNELS TO PROVIDE INSIGHTS FOR LONG RANGE PREDICTION¹

Hans Hallen*, Alexandra Duel-Hallen⁺, Shengquan Hu[^], Tung-Shen Yang⁺, and Ming Lei⁺

*Department of Physics, ⁺Department of Electrical and Computer Engineering and Center for Advanced Computing and Communication, North Carolina State University, Raleigh, NC 27695

[^]Spreadtrum Communications Corp., 4701 Patrick Henry Dr. Building 1401, Santa Clara, CA 95054

ABSTRACT

Algorithms that predict the wireless channel for up to a few wavelengths cannot be adequately tested with stationary models, such as the Jakes model. Moreover, ray-tracing or finite difference time domain (FDTD) methods do not provide insights into the relationship between the reflector configurations and the performance of the long-range prediction. A novel model is required to: (1) create non-stationary datasets to test our previously proposed adaptive long range prediction algorithm, which enables practical realization of adaptive transmission techniques, including modulation, adaptive coding, power control, sentient transmitter diversity, etc. (2) classify the reflector geometries that will have the typical or the most severe parameter variations, so that the reflector configurations for test datasets can be appropriately chosen, (3) provide limits on the speed of adaptation needed for an algorithm to predict the channel significantly into the future, and thereby reveal the timing of future deep fades, etc. and (4) illuminate the origins of the temporal and statistical properties of measured data. We present a model that satisfies these criteria. The algorithm performs similarly on channels given by the physical model or actual measured data, but differently when the channel simulated by the Jakes model. We verify that the insights of the model accurately describe the performance of the algorithm in several scattering environments when prediction is employed with adaptive power control and adaptive modulation. Moreover, we study limits of the long-range prediction at frequencies other than the observed frequency, of importance in correlated uplink and downlink transmission, orthogonal frequency division multiplexing (OFDM) and frequency-hopping systems.

1. INTRODUCTION

The tremendous growth in demand for wireless communications capacity has created a need for new modulation, coding and detection methods that more efficiently use the multipath fading channels encountered in mobile radio. Since the channel changes rapidly, the

transmitter and receiver are not usually optimized for current channel conditions, and thus fail to exploit the full potential of the wireless channel. Recently, several new adaptive transmission techniques [1,2], such as adaptive modulation, adaptive channel coding, adaptive power control, and adaptive transmitter antenna diversity, have been investigated by many researchers. By taking advantage of the time-varying nature of the wireless channels, these adaptive schemes try to use both power and spectrum more efficiently to realize the higher bit rate transmission without sacrificing the Bit Error Rate (BER) performance. To implement adaptive transmission methods in practice, channel state information (CSI) for a future block from tens to hundreds of data symbols must be available at the transmitter due to the feedback delay and other constraints [1]. At realistic mobile speeds, even a small delay will cause a significant degradation of performance, since channel variation for high Doppler shifts usually results in a different received power at the time of transmission than at the time of channel estimation. Therefore, to realize the potential of adaptive transmission methods, the channel variations have to be reliably predicted at least several milliseconds ahead. Recently, we investigated a novel adaptive long-range fading channel prediction algorithm and applied it in adaptive modulation and transmitter diversity [1]. It was demonstrated that this method can forecast the wireless channel well beyond the coherence time, and provides enabling technology for adaptive transmission. (Also, see [1] for references on fading channel prediction.)

In this paper, we describe a novel deterministic fading channel model, and verify that this model will generate realistic fading datasets to test both our prediction algorithm and its application in adaptive transmission schemes. We give examples to illustrate that the insights obtained from the model result in creation of typical and challenging environments for testing prediction performance.

¹ This work was supported by NSF grant CCR-9815002 and ARO grant DAA 19-01-1-0638.

2. THE PHYSICAL MODEL

A well-known statistical model that characterizes a flat fading channel is Rayleigh fading, in which the fading coefficients are modeled as complex Gaussian random variables [3, 4]. The deterministic Jakes model [3] is used as a standard model in computer simulations. However, neither this model nor the depiction as a stationary Rayleigh random process captures the variation of channel parameters associated with each reflected wave (amplitudes, frequencies and phases). The performance of the long-range prediction algorithm [1] depends on this time variation [1, 5-9]. Thus, to test the long-range prediction algorithm and its application in adaptive transmission systems for realistic mobile radio channels, non-stationary data sets are necessary. Long-range prediction is strongly dependent on the short-term fading, so we cannot average it away as is usually done in long-distance (log-normal) fading studies. Further, we are not concerned with modeling the long-distance fading, since it does not qualitatively affect the local flat fading (we can take into account local shadowing of sources, which is important). We are concerned with insights that differentiate typical vs. challenging cases for the prediction. Our model provides these insights, as we demonstrate below, which gives it an advantage over ray-tracing or FDTD models that produce an accurate field value, but little qualitative insights for model testing.

The physical model used is based upon the method of images combined with diffraction theory. An aperture in the object plane defines the object and acts as a source of diffraction. Alternatively, the aperture can be used to shadow a distant reflector, providing accurate local diffraction when the object size would not affect the illumination of the calculation region. The placement of the effective (image) source is determined by the object curvature. [10] Complex objects can be represented as several flat or curved objects with adjacent apertures. The Fresnel diffraction formalism with point-illumination [11] is used to calculate the field for each reflector in the region of interest. The interference pattern c (coherent sum of the complex electric fields E_j of wavelength λ) generated by N plane-wave reflectors with amplitude A_j , (Doppler) frequency f_j and phase ψ_j , and time averaged over an optical cycle, can be written as:

$$\text{Pattern} = c(t) = \sum_{j=1}^N E_j = \sum_{j=1}^N A_j e^{-2\pi i f_j t + i \psi_j}, \quad (1)$$

$$E_j = \left(\frac{i \partial \mathfrak{R} E_{in} e^{-2\pi i \tilde{r}_j / \lambda + i \phi}}{2} \frac{|\mathbf{r}_{scatt} - \mathbf{r}_{effscatt}|}{r} * [C(w_{x2}) - C(w_{x1}) - iS(w_{x2}) + iS(w_{x1})] \right)_j$$

$$* [C(w_{y2}) - C(w_{y1}) - iS(w_{y2}) + iS(w_{y1})]_j$$

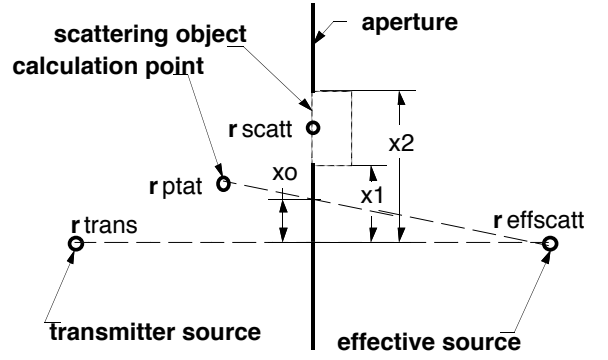


Figure 1. The parameters used to calculate the amplitude from one reflecting object, shown as a dotted rectangle. Also shown is the aperture chosen. The origin is arbitrary since only differences between the vectors are used.

with $w_x = \sqrt{\frac{2}{\lambda \rho}} (x - x_0)$, C and S the Fresnel integrals

$$C(w) = \int_0^w \cos(\pi u^2 / 2) du \quad \text{and} \quad S(w) = \int_0^w \sin(\pi u^2 / 2) du,$$

$$\text{and} \quad \frac{1}{\rho} = \frac{1}{|\mathbf{r}_{scatt} - \mathbf{r}_{effscatt}|} + \frac{1}{|\mathbf{r}_{ptat} - \mathbf{r}_{scatt}|}.$$

All variables refer to the j -th reflector. The parameters and position vectors $\mathbf{r}_{scatt\ j}$, $\mathbf{r}_{effscatt\ j}$, $\mathbf{r}_{ptat\ j}$, x_{1j} , x_{2j} and $r_j = |\mathbf{r}_{ptat} - \mathbf{r}_{effscatt}|_j$ are defined in Figure 1. The reflector at $(\mathbf{r}_{scatt})_j$ has reflectivity \mathfrak{R}_j , and incident power from the transmitter $(E_{in})_j$. The phase factor, $e^{-2\pi i \tilde{r}_j / \lambda + i \phi}$, contains the propagation term proportional to \tilde{r}_j and the phase from the reflection process, ϕ_j . The propagation term \tilde{r}_j is simply r_j for a flat reflector, but needs to be increased by $|\mathbf{r}_{trans} - \mathbf{r}_{scatt}|_j - (\text{curvature radius})_j$ for a curved reflector. The phase ϕ_j could be calculated with the Fresnel formulae, [11], but we treat as a constant without qualitatively altering the result.

To create a dataset, the user of the model specifies the location of the transmitter and the centers of the relevant object surface and aperture (the same when shadowing is not relevant) for each object. The orientation of the aperture, object reflectivity, object curvature, and reflection phase shift are also specified for each object. An aperture is specified for the transmitter so that non-line-of-sight regions can be modeled. Other inputs to the modeling program include the carrier frequency and region of interest (location, size and number of points for each of the two dimensions). The region of interest may be any rectangular array of points from a square to a single line in either direction.

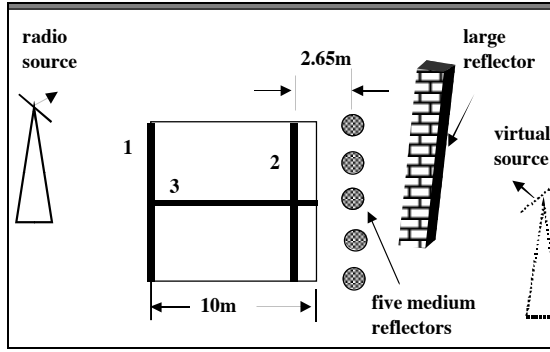


Figure 2 Possible geometry for the physical channel model calculation, with one large and five curved reflecting objects. The virtual source for the large reflector is shown at the right. Those for the curved reflectors are inside the reflectors. The path marked 1 is typical, while those marked 2 and 3 are challenging.

The physical model has the advantage of giving significant insights for determination of typical and challenging-case reflector geometry. The insights derive from the simple relation between the field contribution from each component and the (effective) point source and aperture response in the model. This information is useful for constructing test datasets for algorithms, because it allows a sentient choice of object placement.

For example, the model dataset [5] in Figure 2 was used to examine the effect of variation of the Doppler shifts f_j and other parameters in (1) on prediction performance. The Doppler shift varies with position, most rapidly as the mobile passes the virtual image source and faster when the virtual source is closer. Route 2 in Fig. 2 passes close to the curved objects, so those components of the interference pattern will have relatively rapid Doppler frequency variations (up to 890 Hz/second). This variation causes this route to be a challenging case as discussed below. In contrast, the rate of Doppler frequency variation along route 1 is <200 Hz/second, which is more typical in practice. Path 3 is challenging since the amplitudes of the reflections from the curved reflectors varies quickly ($1/r$) in addition to the Doppler shifts changing. Moreover, it will be shown in Section 3 that for frequency selective channels, variation of the path length differences (excess delays) [4] for various reflected components affects prediction accuracy. Excess delays can also be extracted from physical model scenarios to design typical and difficult tracking conditions. The model provides the ability to vary the excess time delay profile along the path of the mobile in a realistic manner.

3. LONG RANGE PREDICTION OF MODEL AND MEASURED DATA

The ultimate purpose of the model is to provide a testbed for our long-range prediction algorithm. In Figure 3, we

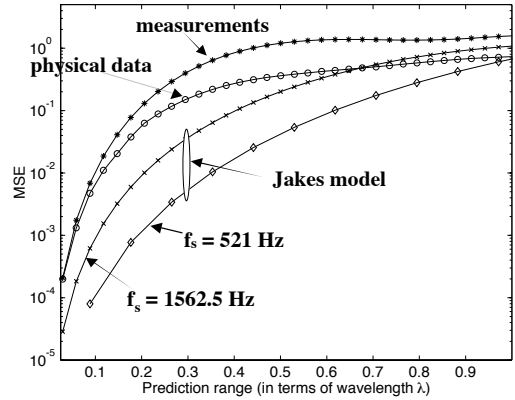


Figure 3. Mean square error of the prediction for Jakes model, physical data and measured data are given as a function of prediction range in wavelengths. ($p = 40$, the maximum Doppler shift $f_{dm} = 46$ Hz, and the sampling rate is 1562.5 Hz).

show the importance of using a nonstationary channel model for testing the prediction algorithm. The complex fading coefficients are predicted using the adaptive long-range prediction method [1]. The prediction algorithm uses an autoregressive (AR) model

$$\hat{c}_n = \sum_{j=1}^p d_j c_{n-j}, \quad (2)$$

where \hat{c}_n is the predicted sample, and c_{n-j} are the observed samples of $c(t)$ in (1). When the channel is given by the sum of several important reflectors, (1), the AR model coefficients d_j in (2) are related to the Doppler frequencies associated with reflectors, whereas the amplitude and phase of each reflector are accounted for through the use

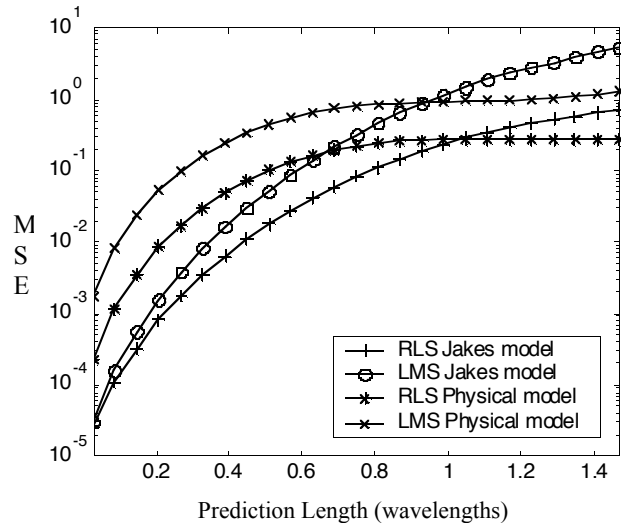


Figure 4. Comparison of prediction mean square error for RLS and LMS with Jakes model and physical model data. The initial observation interval is 500 samples during which LMS is pre-trained to aid convergence. Maximum Doppler shift is 46 Hz, sampling frequency is 1562.5 Hz, and the model order, in (2), is $p=40$.

of the prior data in the prediction [6,12]. The model coefficients d_j are tracked using the Least Mean Squares (LMS) method. Fig. 4 shows that the mean square error (MSE) can be further improved if Recursive Least Squares (RLS) tracking is utilized [10]. The mean square error vs. prediction range is shown for the measured data, our physical model, and the Jakes model. The measured data were collected by a van along a route in low density urban Stockholm. The Jakes, physical model and measured data sets all have similarly shaped autocorrelation functions. Also shown in Figure 3 are the simulation results of MSE vs. prediction range for the Jakes model at a lower sampling rate $f_s=521\text{Hz}$ for the c_n in (2). We found that the prediction of the stationary Jakes model data set can be improved by using a lower sampling rate. The prediction for the non-stationary measured and modeled data is not improved, although it still benefits from a sampling rate much lower than the data rate given a fixed model order [1]. The significant degradation of the MSE for two realistic data sets relative to the Jakes model at shorter prediction lengths is due to the non-stationarity encountered in mobile radio channels. Prediction at the longer ranges depends strongly on the number of important reflectors (fixed in Jakes model, varies for the physical model and measured data) and their variations.

We compared the BER performance of the truncated channel inversion adaptive power control method (TCI) [2] with long-range prediction between typical and challenging cases in Figure 5. Two thresholds, 0.4 and 0.1, are used for the TCI as described in [12]. The channel sampling rate is 1000 Hz and the Maximum Doppler shift 67 Hz. The data rate is 50 Kbps. The simulation utilized 2-step (2 ms) ahead prediction. Typical and challenging datasets correspond to routes 1 and 2 in Figure 2, respectively. The performance difference shows that our physical model insights can help to create different mobile radio environments that both test the limits of the

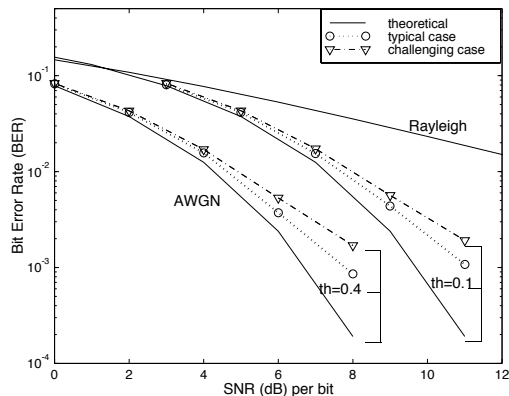


Figure 5. BER performance of TCI for typical and challenging case mobile radio environments is compared. (2ms ahead prediction, $f_{dm}=67\text{Hz}$)

prediction method and validate its application in adaptive power control.

We have investigated adaptive modulation enabled by long-range prediction in [1,8,13]. The basic idea of adaptive modulation [2] is to vary the power and constellation size according to the instantaneous channel condition, which can be measured as either the signal-to-noise (SNR) ratio or the fading gain. We set the target $BER_g = 10^{-3}$, and use fixed power variable rate square M-quadrature amplitude modulation (MQAM) constellations of sizes $M = 0, 2, 4, 16, 64$. Threshold choice based on the predicted channel coefficient and its accuracy was discussed in [8]. In Figure 6, the bit rate of adaptive modulation is compared for the Jakes model, physical model and measured data. Note that our physical model accurately predicts the performance expected under actual conditions, since the prediction performance with model data is similar to that for measured data. Comparison of the three curves reveals that the non-stationarity limits performance of adaptive modulation as the prediction range increases. We found that the bit rate loss is about half a bit for non-stationary data relative to the stationary case. Although the non-stationarity results in reduction of the bit rate relative to the ideal case when the long-range prediction is employed, the bit rate is still significantly larger than when outdated CSI is used to calculate the threshold (over 1 bit/symbol) [8,14].

We extended the adaptive modulation study to systems that use more than one carrier frequency in [13]. The aim is to determine the practicality of observing the signal at one frequency, and adapting signaling requirements at another frequency. In this paper, these frequencies are separated by $\Delta f = 50\text{kHz}$. We generate challenging and

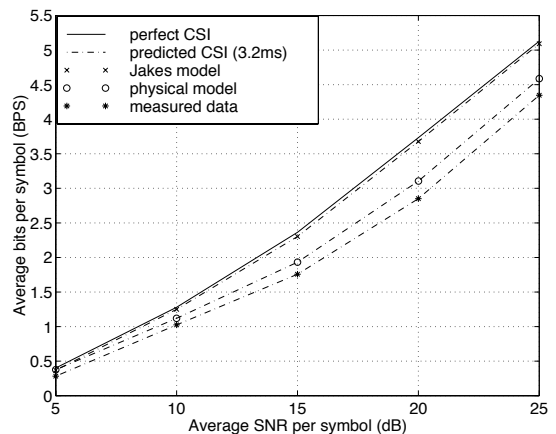


Figure 6. Comparison of average bit rate performance of adaptive modulation for *stationary* data (Jakes model) and *non-stationary* data (physical model and measured data) 3.2ms ahead prediction, target $BER = 10^{-3}$, $f_{dm}=46\text{Hz}$.

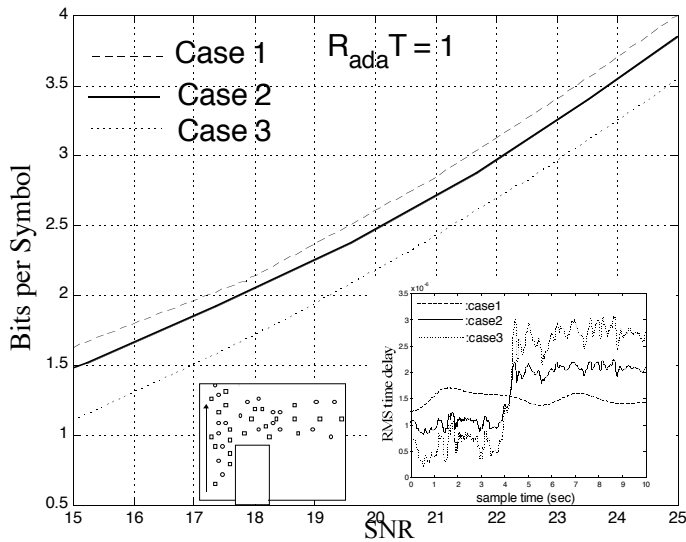


Figure 7. Bits per symbol at various SNRs are shown for three cases exhibiting different RMS delay spread variation rates (right inset), the latter two from a shadowing scenario (left inset). Case1: flat rms distribution, mean = 1.5 μ s, case 2: rms from 0.7 μ s to 2.3 μ s, case 3: rms from 0.4 μ s to 2.6 μ s.

typical case scenarios for this purpose. In Figure 7, reflectors are arranged to give an excess delay distribution that is approximately exponential [3,13], characterized by the rms delay spread [4]. The rms value is usually very slowly varying (case 1), although near a shadowing structure (left inset of Fig. 7), the delay spread can vary rapidly (right inset), cases 2 and 3. We investigate the performance of adaptive modulation on these channels during the $T = 1$ s interval when the rms varies in cases 2 and 3 (from 3.5 to 4.5 s in the right inset). The value of the rms is not updated during this interval. The target BER = 10^{-3} , and continuous power variable rate MQAM method with the same modulation levels as above is used. The result shows the 2dB loss for the challenging case 3 relative to the rms-invariant case. To improve performance, the rms value needs to be tracked and updated (the adaptation rate is denoted R_{ada}). For challenging cases, an acceptable $R_{ada}T = 5$ is required to avoid performance loss.

CONCLUSIONS

We have presented an overview of a physical model that generates realistic, non-stationary data for long-range prediction testing, and provides expectations of the degree of prediction difficulty for various environments. It allows calculation of the rates at which parameters associated with the reflectors vary, and hence the adaptive tracking speed required to accurately predict future channel properties. The channel prediction methods tested here perform similarly with both the non-stationary channel generated by the model and with measured channel data.

The application of the channel prediction method for adaptive power control and adaptive modulation is validated with our physical model for typical and challenging propagation environments.

ACKNOWLEDGMENT

The authors would like to thank Jan-Eric Berg and Henrik Asplund of Ericsson, Inc. for providing the measured data.

REFERENCES

- [1] A. Duel-Hallen, S. Hu, H. Hallen, "Long-range Prediction of Fading Signals: Enabling Adaptive Transmission for Mobile Radio Channels", *IEEE Signal Processing Magazine*, Vol. 17, No.3, pp. 62- 75, May 2000.
- [2] A. J. Goldsmith and S. G. Chua, "Variable-Rate Variable-Power MQAM for Fading Channels", *IEEE Trans. Commun.* vol. 45, No. 10, pp. 1218 - 1230, Oct. 1997.
- [3] W. C. Jakes, Jr., *Microwave Mobile Communications*. New York: Wiley, 1974.
- [4] T. S. Rappaport, *Wireless Communications: Principles and Practice*, Prentice Hall, 1996.
- [5] S. Hu, H. Hallen and A. Duel-Hallen, "Physical Channel Modeling, Adaptive Prediction and Transmitter Diversity for Flat Fading Mobile Channels," *Proceedings of SPAWC'99*, May 1999, pp.387-390.
- [6] Eyceoz, A. Duel-Hallen, and H. Hallen "Prediction of Fast Fading Parameters by Resolving the Interference Pattern", *Proceedings of the 31st ASILOMAR Conference on Signals, Systems, and Computers*, Nov. 2-5, 1997.
- [7] T. Eyceoz, S. Hu, and A. Duel-Hallen, "Performance Analysis of Long Range Prediction for Fast Fading Channels", *Proc. 33rd Annual Conference on Information Sciences and Systems CISS'99*, March 1999, pp.656-661 .
- [8] S. Hu, A. Duel-Hallen, H. Hallen, "Long Range Prediction Makes Adaptive Modulation Feasible in Realistic Mobile Radio Channel," *Proc. 34rd Annual Conference on Information Sciences and Systems CISS'2000*, March 2000, Volume I, pp.WP4.7-12.
- [9] S. Hu, A. Duel-Hallen, H. Hallen, "Selective Transmitter Diversity and Adaptive Power Control for Realistic Mobile Radio Channels," *IASTED International Conference on Wireless and Optical Communications (WOC 2001)*, Banff, Canada, June 27-29, 2001.
- [10] H. Hallen, S. Hu, M. Lei and A. Duel-Hallen, "A Physical Model for Wireless Channels to Understand and Test Long Range Prediction of Flat Fading," *Proceedings of WIRELESS 2001*, Calgary, Canada, July 9-11, 2001, pp. 99-107.
- [11] R.D. Guenther, *Modern Optics*, New York, Wiley, 1990.
- [12] T. Eyceoz, A. Duel-Hallen, H. Hallen, "Deterministic Channel Modeling and Long Range Prediction of Fast Fading Mobile Radio Channels," *IEEE Commun. Lett.*, Vol. 2, No. 9, pp. 254 - 256, Sept. 1998
- [13] T. S. Yang, A. Duel-Hallen, "Adaptive Modulation Using Outdated Samples of Another Fading Channel," *Proceedings of WCNC'02*, Orlando, FL, March 17-21, 2002
- [14] D. L. Goeckel, "Adaptive Coding for Fading Channels using Outdated Channel Estimates", *Proc. VTC*, May 1998.